Pakistan J. Zool., vol. 48(1), pp. 151-157, 2015.

De Novo Characterization of Velvet Skin Transcriptome at the Antlers Tips of Red Deer (*Cervus elaphus*) and Analysis of Growth Factors and Their Receptors Related to Regeneration

Xiaoguang Yang†, Yanxia Chen†, Xuedong Liu, Qingzhen Liu, Xiaomeng Pi, Yuhui Liu and Dong Zheng*

Laboratory of Genetics and Molecular Biology, Northeast Forestry University, Harbin 150040, P.R. China

†X. Yang and Y. Chen contributed equally to the article.

A B S T R A C T

The regeneration of antler velvet represents a new form of stem-cell-derived full skin regeneration, including associated appendages. While much is known of the morphological changes involved in this process, transcriptome data are lacking. In this study, we performed *de novo* transcriptome assembly and analysis of 27.44 million clean short reads for regenerating velvet skin in red deer (*Cervus elaphus*) using RNA-sequencing technology. These reads were assembled into 68,924 unique sequences. Based on BLASTX alignment, we identified 33,471 distinct transcripts. Assembled sequences were then annotated using Gene Ontology terms, Clusters of Orthologous Groups classifications, and the Kyoto Encyclopedia of Genes and Genomes. Of the 33,471 annotated sequences, 9,252 sequences were categorized into 52 GO functional groups, and 11,428 sequences had a COG classification. In total, we assigned 25,577 of the annotated sequences to 241 KEGG pathways. We found a number of highly expressed genes, including collagens, ribosomal proteins, growth factors, growth factors receptors, and extracellular matrix proteins. The data generated in this study represent the most comprehensive sequence resource available for regenerating velvet skin in red deer antlers and provide a basis for further research on deer antler molecular genetics and functional genomics.

Article Information

Received 22 May 2014
Revised 4 July 2015
Accepted 25 August 2015
Available online 1 January 2016

Authors' Contributions

XY, YC and DZ designed the experiments, XY, XL, QL and XP performed the experiments, YC, XL and YL analyzed the data, XY, YC and DZ wrote the paper.

Key words

Antler velvet skin, red deer, regeneration, transcriptome, growth factors.

INTRODUCTION

Antlers are the only appendages capable of regeneration in mammals, and are one of the fastest growing organs, capable of growing up to 2 cm per day (Li, 2012). Initiation of antler growth takes place at the bone appendix (pedicle), starting on the frontal bone, which is covered with antlerogenic periosteum (Price and Allen, 2004). Both pedicles and regenerating antlers contain internal (cartilage and bone) and external (skin, blood vessels, and nerves) tissue components (Li, 2010). However, studies have shown that the external tissue components of antlers are not simple extensions of their pedicle counterparts. Pedicles and antlers are distinguished by skin type: pedicles are enveloped by typical scalp skin, while antlers have a unique 'velvet' skin that is sparsely populated with hair (Li *et al*., 2013). Regeneration of velvet skin commences when the wound over a pedicle stump heals via distal pedicle skin. Wound healing is an obligatory process that restores continuity of interrupted tissue (Goad *et al*., 1996). The process is unique because as the centripetally migrating healing skin passes the distal pedicle periosteum (PP) the skin changes from the scalp to the velvet type. In contrast to pedicle skin (a typical scalp skin), antler velvet lacks a subcutaneous loose connective tissue layer, and instead has a thicker epidermis and the ability to form new hair follicles. These newly formed follicles lack associated arrector pili muscles and sweat glands but possess large multi-lobed sebaceous glands (Li, 2010). These histological features make velvet a unique skin type and suggest that large-scale changes in gene expression have occurred to generate this novel structure, via a series of proliferation, patterning, and differentiation events. However, to date, little is known about the gene expression patterns underlying the generation of antler velvet.

The recent development of next-generation sequencing technology can provide information on gene expression that is independent of any knowledge of genomic sequences. It also offers greater sensitivity and a larger dynamic range of gene expression than do array-based technologies (Marioni *et al*., 2008). The RNA-

* Corresponding author: zhengdong89@yeah.net
0030-9923/2016/0001-0151 $ 8.00/0

sequencing method (RNA-Seq) was originally developed to take advantage of the next-generation Illumina sequencing technology and improve annotation of the yeast genome and explore its transcriptional expression profile (Nagalakshmi *et al*., 2008). This method exhibits relatively little variation among technical replicates, which is advantageous for identifying expressed genes networks (Marioni *et al*., 2008). RNA-Seq has been applied to answer questions regarding comprehensive transcriptomic analyses in several species (Capobianco, 2014), but has not, to our knowledge, been applied to create a gene expression atlas of regenerating antler velvet in red deer (*Cervus elaphus*).

In this study, we used Illumina technology to generate over 27 million high-quality reads of cDNA sequence from velvet skin from the growing antler tip of the red deer, which we assembled, classified based on gene association pathways, and evaluated expression patterns. This information greatly enhances our understanding of the mechanism underlying the formation of velvet skin, and of mammalian regenerative processes more generally.

MATERIALS AND METHODS

Sample collection and preparation

All experimental procedures were approved by the Animal Ethics Committee of Northeast Forestry University (Permit Number: 2012-0016). We followed the protocol of Li *et al*. (2002) for removal of antlers. Antler tips in the rapid growth period (60 days after the previous hard antlers had been cast off) were collected from three anesthetized 3-year-old captive red deer held at the Qinghuangdao Safari, China. The velvet skin was removed from the growth tips, cut into small pieces, and immediately stored in liquid nitrogen for further processing.

RNA isolation and library preparation for transcriptome analysis

We used the SV Total RNA Isolation System (Promega, Madison, WI, USA) to isolate total RNA according to the manufacturer's instructions. RNA integrity was evaluated by gel electrophoresis, while RNA purity was checked by examining the ratio of OD_{260}/OD_{280} and the RNA Integrity Number (RIN) value. RNA samples with RIN values >7.5 and OD_{260}/OD_{280} ratios >1.9 were selected for deep sequencing. We pooled total RNA samples from the three individuals before mRNA isolation. Next, we used the FastTrack MAG mRNA Isolation Kit (Invitrogen) to purify mRNA from 10 mg of total RNA. The isolated mRNA was fragmented and then first-strand cDNA synthesis was undertaken using random hexamer-primers. Second-strand cDNA was synthesized using buffer, dNTPs, RNase H, and DNA polymerase I. The short cDNA fragments were purified using QiaQuick PCR extraction kit (Qiagen, Uesseldorf, Germany). The fragment ends were repaired and A-tailed, and then ligated to sequencing adaptors.

Deep sequencing, de novo *assembly, and gene expression level analysis*

We used the Illumina Hiseq 2000 platform to sequence the cDNA library. Reads were assembled using Trinity (Grabherr *et al*., 2011). The longest assembled sequences are called contigs. We mapped reads back to contigs. Using paired-end reads, this system is able to detect contigs from the same transcript and discern the distances between them. Finally, we obtained sequences without Ns that could not be extended on either end, known as unigenes. Where there were several samples from the same species, TGICL (Pertea *et al*., 2003) was used to assemble all the unigenes from different samples to form a single set of non-redundant unigenes. Gene expression level analysis was performed by the reads per kilobase per million mapped reads (RPKM) method using the formula $RPKM = 10^3C/NL$, where C is the number of mappable reads that uniquely align to a unigene, N is the total number of mappable reads that uniquely align to all unigenes, and L is the sum of the unigenes in base pairs (Mortazavi *et al*., 2008).

BLAST homology search, functional annotation, and gene expression level analysis

To determine the homology of sequences with known genes, distinct sequences were used in a BLASTX search and annotated against the National Centre for Biotechnology Information (NCBI) non-redundant database (E value 10^{-5}). Functional annotation by Gene Ontology (GO) terms was performed using Blast2go software (http://www.blast2go.com) against the GO database (Conesa and Gotz, 2008). Annotation with the COG and KEGG pathways was conducted using BLASTX against the COGs database (Tatusov *et al*., 2001) and the *Kyoto Encyclopedia of Genes and Genomes* database (Kanehisa *et al*., 2004).

Validation of mRNA expressed in velvet skin of Red deer

Six fibroblast growth factor and two fibroblast growth factor receptor genes were selected for validation by real-time qPCR analysis. Pooled mRNA (1 µg) was converted to cDNA using oligo dT primer and MMLV cDNA kit mix (New England Biolabs, Ipswich, MA, USA). The cDNA was then used for real-time qPCR using mRNA specific primers (Supplementary Table S1). The 10-µL PCR reaction contained 5 µL SYBR Premix

Ex TaqTM II (Takara, Dalian, China), 0.5 µL specific forward primer, 0.5 µL reverse primer, 0.5 µL ROX reference dye, 2 µL diluted (2 times) cDNA, and 1.5 µL water. Cycling parameters were 94°C for 30 s, followed by 60 cycles of 94°C for 5 s followed by 60°C for 40 s. Melting curve analyses were performed following amplifications. All reactions were performed six times on the Mastercycler EP Realplex system (Eppendorf). The gene expressions of target genes were normalized against the endogenous control, 7SL RNA. The relative gene expression was calculated using the comparative C(T) method (Schmittgen and Livak, 2008).

RESULTS

Illumina sequencing, de novo *assembly, and sequence analysis*

To create an atlas of gene expression in rapidly growing velvet skin, we prepared a cDNA library for the Illumina sequencing. After cleaning and quality checks, we obtained 27 million reads, each of 90 bp (NCBI SRA Accession No. SRR2068609). Over 96% of these reads had quality scores at the Q20 level (i.e. a base quality >20 and an error probability of 0.01).

De novo assembly of the clean reads by Trinity (http://trinityrnaseq.sourceforge.net/) resulted in 111,928 contigs with an N50 of 752 bp (50% of the assembled bases were incorporated into contigs of 752 bp or longer; mean contig size = 401 bp, range = 48–6,361 bp; Table I). The 111,928 contigs generated 68,924 unigenes with a mean size of 657 bp and an N50 of 1106 bp (Table I).

Table I.- Overview of the results of sequencing and assembly.

Feature	Statistics
Total number of reads	27,442,748
Total base pairs (bp)	2,469,847,320
Average read length (bp)	90
Total number of contigs	111,928
Mean length of contigs (bp)	401
N50 of contigs (bp)	752
Total number of unigenes	68,924
Mean length of unigenes (bp)	657
N50 of unigenes (bp)	1106

Functional annotation of the unigenes

Distinct unigenes were searched using BLASTX against the NCBI nr database (with an E-value of 10^{-5}). Using this approach, 33,471 genes (48.6% of all unigenes) returned a BLAST result above the cut-off value. Because of a lack of genome and expressed sequence tags (EST) information for Red deer, 51.4% of unigenes could not be matched to known genes. Similarly, up to 36,162 unigenes (52.5% of all unigenes) had no Swissprot annotation. Based on GO classifications, 9,252 sequences were categorized into 52 functional groups (Fig. 1). In the three GO terms (biological process, cellular component, and molecular function), ‘cell’ (7,687 members), ‘cell part’ (7,380 members) and ‘cellular process’ (5,781 members) were, respectively, the most frequently used three terms. Few genes were found in the categories of ‘antioxidant activity’ (three members) and ‘metallochaperone activity’ (one member; Fig. 1).

Of the 33,471 annotated sequences, 11,428 sequences had a COG classification (Fig. 2). Among the 25 COG categories, ‘general function prediction only’ was the largest represented group (4,483 members), while ‘nuclear structure’ was the smallest (4 members; Fig. 2). In total, we assigned 25,577 of the annotated sequences to 241 KEGG pathways (Supplementary Table S2). The pathways with the most representation among the unique sequences were the metabolic pathways (2,325 members).

Highly expressed genes involved in antler velvet regeneration

The 50 most expressed genes in velvet skin included genes belonging to the ribosomal protein and collagen families (Table II). The most highly expressed gene was the collagen alpha-1(I) chain. The other highly expressed genes included, collagen alpha-2(I) chain, acidic cysteine-rich secreted protein, cytochrome c oxidase subunit I, NADH dehydrogenase subunit 1, thymosin, beta 10, acidic ribosomal phosphoprotein PO, uteroferrin-like, ubiquitin, translationally controlled tumor protein 1, elongation factor 1-alpha 1, ferritin light chain-like and senescence-associated protein. The list of the most highly expressed genes also included one *Drosophila* GI14048 homology transcript.

We selected six fibroblast growth factor genes and two fibroblast growth factor receptor genes from which we designed eight primer pairs for qPCR validation (Supplementary Table S1). The results showed consistent expression patterns with the observed findings in transcriptome analysis (Supplementary Fig. S1). This agreement indicated that the abundance of the Illumina sequences from the Red deer transcriptome closely mirrored actual expression levels.

Growth factors and their receptors involved in antler velvet regeneration

In the transcriptome of velvet skin, there were at least 70 genes encoding growth factors (44 members;

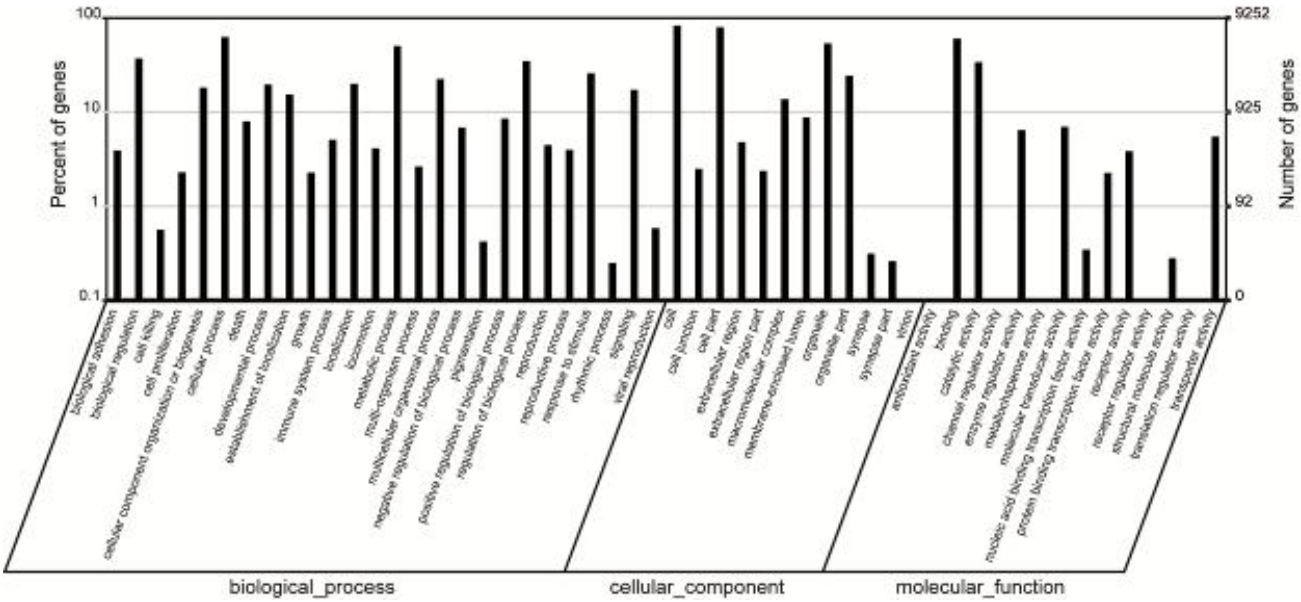

Fig. 1. Gene Ontology functional classifications of all unigenes identified in regenerating velvet skin of Red deer (*Cervus elaphus*) antlers.

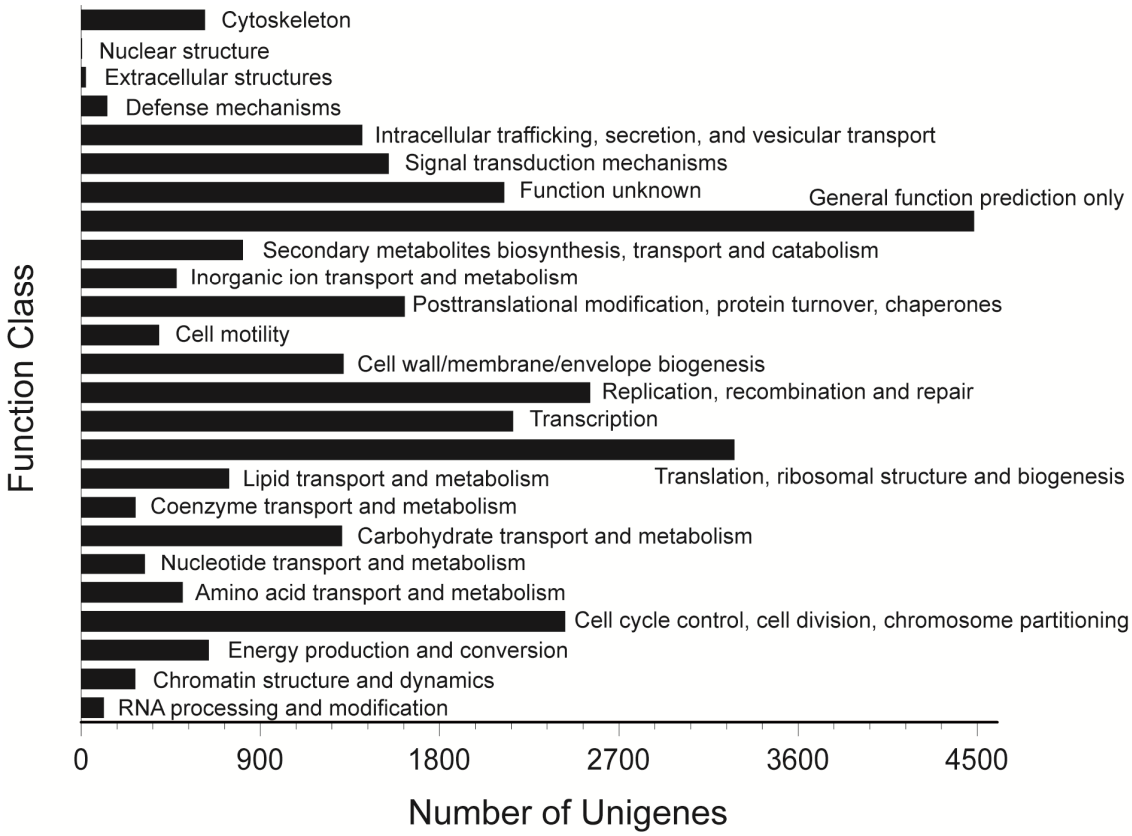

Fig. 2. Clusters of Orthologous Groups functional classifications of all unigenes identified in regenerating velvet skin of Red deer (*Cervus elaphus*) antlers.

Table II.- Details of the 50 most highly expressed genes in regenerating velvet skin of Red deer (*Cervus elaphus*) antlers.

Gene name	RPKM[a]
Collagen alpha-1(I) chain	13740.43
Collagen alpha-2(I) chain	11033.75
Secreted protein, acidic, cysteine-rich (osteonectin), isoform CRA_a	7154.04
Cytochrome c oxidase subunit I	6600.02
NADH dehydrogenase subunit 1	5327.62
PREDICTED: 60S ribosomal protein L37-like	4206.55
PREDICTED: 60S acidic ribosomal protein P1-like	3931.70
PREDICTED:collagen alpha-1(II) chain	3584.78
40S ribosomal protein S11	2960.59
PREDICTED: 40S ribosomal protein S18-like isoform 1	2901.41
Thymosin, beta 10, isoform CRA_a	2642.68
PREDICTED: 40S ribosomal protein S15a-like	2632.45
Acidic ribosomal phosphoprotein PO	2615.88
Ribosomal protein L35-like	2381.67
PREDICTED: 40S ribosomal protein S20-like isoform 2	2317.62
PREDICTED: 40S ribosomal protein S29-like	2210.28
Uteroferrin-like	2179.85
Collagen alpha-1(III) chain	2164.91
Ubiquitin	2061.02
PREDICTED: ubiquitin-60S ribosomal protein L40-like	2029.89
40S ribosomal protein S8	1928.11
PREDICTED: 60S ribosomal protein L17-like	1904.49
40S ribosomal protein S15	1903.38
Tumor protein, translationally-controlled 1	1900.65
60S ribosomal protein L18	1896.79
Elongation factor 1-alpha 1	1879.42
40S ribosomal protein S2	1863.65
60S ribosomal protein L4	1842.22
Ferritin light chain-like	1816.21
40S ribosomal protein S26	1804.48
40S ribosomal protein SA	1774.72
PREDICTED: similar to ribosomal protein L18a isoform 1	1769.93
60S ribosomal protein L13a	1753.49
60S ribosomal protein L5	1734.24
Senescence-associated protein	1725.64
mCG7861, isoform CRA_b	1724.24
Collagen alpha-1(II) chain isoform 2	1721.41
PREDICTED: 60S ribosomal protein L31-like	1625.68
Peptidylprolyl isomerase A-like, isoform CRA_c	1611.53
PREDICTED: guanine nucleotide-binding protein subunit beta-2-like 1-like	1610.78
GI14048 homology	1547.85
mCG19129	1520.62
PREDICTED: 40S ribosomal protein S14-like	1498.49
60S ribosomal protein L10a	1492.80
PREDICTED: rRNA promoter binding protein-like	1490.12
Fatty acid 2-hydroxylase	1485.47
60S ribosomal protein L6	1481.68
Cystatin-M	1476.81
60S ribosomal protein L27	1443.36
Ribosomal protein P2-like	1435.19

[a]Refers to reads per kilobase per million mapped reads

Supplementary Table S3) and their receptors (26 members; Supplementary Table S4). The highly expressed growth factor genes in velvet skin included insulin-like growth factor 2 (IGF2) isoform 3, transforming growth factor beta-1, connective tissue growth factor, heparin-binding growth factor 8, hepatoma-derived growth factor, vascular endothelial growth factor B, and stem cell growth factor. The highly expressed growth factor receptor genes, meanwhile, were platelet-derived growth factor receptor-like protein, platelet-derived growth factor receptor (beta polypeptide), autocrine motility factor receptor, transforming growth factor beta type 2 receptor, epidermal growth factor receptor, and insulin-like growth factor 2 receptor (IGF2R).

DISCUSSION

Epimorphic organ regeneration involves *de novo* development of appendages distal to the level of amputation (Goss, 1983). Urodele amphibians typify the traditional view of epimorphic regeneration, regenerating many different body structures throughout their lives, including jaws, tail, and limbs (Tsonis, 2000). Unlike urodele limb regeneration, antler regeneration does not involve cell de-differentiation and the formation of a blastema from the de-differentiated cells; rather, antler regeneration appears to a stem-cell-based process that requires the periodic activation of periosteal stem cells of the distal pedicle, which are presumably derived from the neural-crest (Kierdorf *et al*., 2007). Hence, antler regeneration, including the regeneration of velvet skin, is a new form of stem-cell-derived epimorphic regeneration. Interestingly, we still found several skin stem cell markers expressed at lower levels in regenerating velvet, including integrin alpha 6/CD49f, CD200, follistatin, tenascin, YAP1, and the general stem cell marker, CD34 (Blanpain and Fuchs, 2006). These might be expressed by stem cells residing within the so-called ‘bulge’, a niche within the hair follicle. These epidermal stem cells are generally quiescent but can be stimulated to proliferate and differentiate into the specialized cells that compose a hair follicle.

Although the regeneration of antler velvet has been studied extensively at the morphological and histological levels (Bubenik, 1996; Li and Suttie, 2000), trancriptome data for this process are lacking. Illumina RNA-Seq technology is an efficient and cost-effective method for discovering novel genes and investigating gene expression patterns, especially in non-model organisms without sequenced genomes (Shi *et al*., 2011; Hao *et al*., 2012). Using this technique, we obtained a

comprehensive transcriptome atlas for regenerating Red deer velvet skin. We generated 111,928 contigs over 200 bp in length (average contig length 401 bp and N50 length 752 bp), which yielded 33,471 non-redundant accessions, indicating that more than half of the contigs (51.4%) did not belong to known unigene clusters.

Genes encoding for ribosomal proteins were among the most highly expressed genes detected in velvet skin. The ribosome is a central player in the translation system that decodes the nucleotide sequences carried by the mRNA and converts them into their amino acid primary structures. An abundance of ribosomal proteins in velvet skin suggests there are high rates of protein translation occurring in antler velvet. In total, 11 members of the matrix metalloproteinase (MMP) family, each of which cleaves a specific subset of matrix proteins, were also expressed by velvet. The MMPs most heavily induced in velvet skin were MMP9 and MMP14. MMP9 (gelatinase B) can cut basal lamina collagen (type IV) and anchoring fibril collagen (type VII), and is thought to be responsible for releasing keratinocytes from their tethers to the basal lamina (Cirillo *et al*., 2007). Additionally, overexpressed MMP9 might play a role in tumor-associated tissue remodeling (Vandooren *et al*., 2013). Unlike MMP9, MMP14 is a member of the membrane-type MMP (MT-MMP) subfamily. Each member of this subfamily contains a potential transmembrane domain suggesting that these proteins are expressed at the cell surface rather than secreted. This protein also activates MMP2 protein. We found that genes encoding for important oxidative and dehydrolytic enzymes such as NADH1 and COX1 were also highly expressed in velvet skin. The coenzyme NAD (nicotinamide adenine dinucleotide) is a key electron carrier that mediates hundreds of reactions. The redox state of the NAD–NADH couple plays a central role in energy metabolism, signal transduction, and transcriptional regulation (Fan *et al*., 2013), which is consistent with the need for mitochondrial biogenesis, energy, and other proteins during rapid growth of velvet.

Many growth factors and their receptors were enriched in velvet. Among them, insulin-like growth factor 2 (IGF2), instead of insulin-like growth factor 1, was the most highly expressed. This finding supports the consensus view of IGF2 as a major fetal growth factor, with IGF1 being a major growth factor in adults (D'Ercole, 1996). This finding also suggests that IGF2 could be a main hormone regulating velvet regeneration, at least during the 60-day regeneration phase. Accordingly, we also found that insulin-like growth factor 2 receptor (IGF2R), but not insulin-like growth factor 1 receptor (IGF1R), was highly expressed in velvet. IGF2R is a multifunctional protein receptor that binds IGF2 at the cell surface and mannose-6-phosphate (M6P)-tagged proteins in the trans-Golgi network. Interestingly, a study of the mannose-6-phosphate (M6P)–IGFII receptor has suggested that IGF2R was involved in the prevention of scars (Martin, 1997), a phenomenon usually found at the wound healing phase of antler regeneration (Kierdorf *et al*., 2007).

We found that the GO ananlysis of Red deer velvet showed distinct differences in gene expression patterns from those reported for Sika deer (*Cervus Nippon*) (Yao *et al*., 2012). For example, 10 types of GO terms were exclusive to Red deer velvet (cell proliferation, negative regulation of biological process, positive regulation process, regulation of biological process, signaling, cell junction, channel regulator activity, nucleic acid binding transcription factor activity, receptor activity, and receptor regulator activity). Furthermore, five GO terms were entirely absent from red deer velvet (virion part, electron carrier activity, nutrient reservoir activity, proteasome regulator activity, protein tag). These differences in the GO terms for regenerating velvet skin in these two deer species suggest that unique gene networks underlie these processes in a velvet tissue-specific manner.

Many fundamental questions remain to be answered before meaningful progress can be made in understanding antler regeneration. The transcription profile of antler velvet skin during its fast growth phase that we have provided in this study will facilitate future studies on stem-cell-derived skin regeneration. Additionally, the data we have generated in this study will contribute to research investigating regeneration processes for tissue engineering and clinical relevance.

ACKNOWLEDGMENTS

This work was supported by the Fundamental Research Funds for the Central Universities in China (No. 2572014EA05-01) and the Program for New Century Excellent Talents in University of China (No. NCET-11-0609).

Conflict of interest declaration

The authors declare that they have no conflict of interest.

REFERENCES

Blanpain, C. and Fuchs, E., 2006. Epidermal stem cells of the skin. *Annu. Rev. Cell Dev. Biol.*, **22**:339-373.

Bubenik, G., 1996. Morphological investigations of the winter coat in white-tailed deer: Differences in skin, glands and hair structure of various body regions. *Acta Theriol.*,

41:73-82.

Capobianco, E., 2014. RNA-Seq data: a complexity journey. *Comput. Struct. Biotechnol. J.*, **11**:123-130.

Cirillo, N., Lanza, M., Rossiello, L., Gombos, F. and Lanza, A., 2007. Defining the involvement of proteinases in pemphigus vulgaris: evidence of matrix metalloproteinase-9 overexpression in experimental models of disease. *J Cell Physiol*., **212**:36-41.

Conesa, A. and Gotz, S., 2008. Blast2GO: a comprehensive suite for functional analysis in plant genomics. *Int. J. Pl. Genom.*, **2008**:619832.

D'Ercole, A.J., 1996. Insulin-like growth factors and their receptors in growth. *Endocrinol. Metab. Clin. N. Am.*, **25**:573-590.

Fan, R., Xie, J. and Bai, J., 2013. Skin transcriptome profiles associated with coat color in sheep. *BMC Genomics*, **14**: 389-401.

Goad, D.L., Rubin, J., Wang, H., Tashjian, Jr. A.H. and Patterson, C., 1996. Enhanced expression of vascular endothelial growth factor in human SaOS-2 osteoblast-like cells and murine osteoblasts induced by insulin-like growth factor I. *Endocrinology*, **137**: 2262-2268.

Goss, R.J., 1983. *Deer antlers. regeneration, function and evolution*. Academic Press. New York, NY.

Grabherr, M.G., Haas, B.J., Yassour, M., Levin, J.Z., Thompson, D.A., Amit, I., Adiconis, X., Fan, L., Raychowdhury, R., Zeng, Q., Chen, Z., Mauceli, E., Hacohen, N., Gnirke, A., Rhind, N., Di Palma, F., Birren, B.W., Nusbaum, C., Lindblad-toh, K., Friedman, N. and Regev, A., 2011. Full-length transcriptome assembly from RNA-seq data without a reference genome. *Nat. Biotechnol.*, **29**:644-652.

Hao, L., Hu, Y., Xiao, X. and Li, H., 2012. Full length cDNA cloning and expression analysis of calmodulin gene from deer antler tissue. *Pakistan J. Zool*., **44:**1225-1230.

Kanehisa, M., Goto, S., Kawashima, S., Okuno, Y. and Hattori, M., 2004. The KEGG resource for deciphering the genome. *Nucl. Acids Res*., **32**: D277-D280.

Kierdorf, U., Kierdorf, H. and Szuwart, T., 2007. Deer antler regeneration: cells, concepts, and controversies. *J. Morphol*., **268**:726-738.

Li, C., 2010. Exploration of the mechanism underlying neogenesis and regeneration of postnatal mammalian skin—deer antler velvet. *Int. J. Med. Biol. Front*., **16**:1-18.

Li, C., 2012. Deer antler regeneration: a stem cell-based epimorphic process. *Birth Defects Res. C Embryo Today*, **96**:51-62

Li, C., Clark, D.E., Lord, E.A., Stanton, J.A. and Suttie, J.M., 2002. Sampling technique to discriminate the different tissue layers of growing antler tips for gene discovery. *Anat. Rec*., **268**:125-130.

Li, C. and Suttie, J.M., 2000. Histological studies of pedicle skin formation and its transformation to antler velvet in red deer (*Cervus elaphus*). *Anat. Rec.*, **260**:62-71.

Li, C., Pearson, A. and McMahon, C., 2013. Morphogenetic mechanisms in the cyclic regeneration of hair follicles and deer antlers from stem cells. *Biomed. Res. Int*., **2013**:643601.

Marioni, J.C., Mason, C.E., Mane, S.M., Stephens, M. and Gilad, Y., 2008. RNA-seq: an assessment of technical reproducibility and comparison with gene expression arrays. *Genome Res*., **18**:1509-1517.

Martin, P., 1997. Wound healing-aiming for perfect skin regeneration. *Science*, **276**:75-81.

Mortazavi, A., Williams, B.A., McCue, K., Schaeffer, L. and Wold, B., 2008. Mapping and quantifying mammalian transcriptomes by RNA-Seq. *Nat. Methods*, **5**:1-8.

Nagalakshmi, U., Wang, Z., Waern, K., Shou, C., Raha, D., Gerstein, M. and Snyder, M., 2008. The transcriptional landscape of the yeast genome defined by RNA sequencing. *Science*, **320**:1344-1349.

Pertea, G., Huang, X., Liang, F., Antonescu, V., Sultana, R., Karamycheva, S., Lee, Y., White, J., Cheung, F., Parvizi, B., Tsai, J. and Quackenbush, J., 2003. TIGR gene indices clustering tools (TGICL): a software system for fast clustering of large EST datasets. *Bioinformatics*, **19**:651-652.

Price, J. and Allen, S., 2004. Exploring the mechanisms regulating regeneration of deer antlers. *Phil. Trans. R. Soc. Lond B*, **359**:809-822.

Schmittgen, T.D. and Livak, K.J., 2008. Analyzing real-time PCR data by the comparative C(T) method. *Nat. Protoc*., **3**:1101-1108.

Shi, C.Y., Yang, H., Wei, C.L., Yu, O., Zhang, Z.Z., Jiang, C.J., Sun, J., Li, Y.Y., Chen, Q., Xia, T. and Wan, X.C., 2011. Deep sequencing of the Camellia sinensis transcriptome revealed candidate genes for major metabolic pathways of tea-specific compounds. *BMC Genom.*, **12**:131-150.

Tatusov, R.L., Natale, D.A., Garkavtsev, I.V., Tatusova, T.A., Shankavaram, U.T., Rao, B.S., Kiryutin, B., Galperin, M.Y., Fedorova, N.D. and Koonin, E.V., 2001. The COG database: new developments in phylogenetic classification of proteins from complete genomes. *Nucl. Acids Res*., **29**:22-28.

Tsonis, P.A., 2000. Regeneration in vertebrates. *Dev. Biol*., **221**:273-284.

Vandooren, J., Van Den Steen, P.E. and Opdenakker, G., 2013. Biochemistry and molecular biology of gelatinase B or matrix metalloproteinase-9 (MMP-9): the next decade. *Crit. Rev. Biochem. Mol. Biol*., **48**:222-272.

Yao, B., Zhao, Y., Wang, Q., Zhang, M., Liu, M., Liu, H. and Li, J., 2012. *De novo* characterization of the antler tip of Chinese Sika deer transcriptome and analysis of gene expression related to rapid growth. *Mol. Cell Biochem*., **364**:93-100.

SUPPLEMENTARY TABLES

Table S1.- Primers used for quantitative real-time PCR. List of primers for eight genes used in quantitative real-time PCR analysis to verify genes expression identified by RNA-Seq analysis.

Gene names	Primer sequence (5′→3′)
Fibroblast growth factor 5 (FGF5)	F[a]: GCATGAGCTTGTCCTTCCTCCTCC R[b]: TTTGGGTGCGAGGCGCTT
Fibroblast growth factor 7(FGF7)	F: GCCAAGTTTGCTCTACAGA R: ACTTCTTGTATGTCGCTCGG
Fibroblast growth factor 10 (FGF10)	F: AAGAAGGAAAACCGCCCGTA R: TTCCCCTTCTTGTTCATGGCTA
Fibroblast growth factor 11 (FGF11)	F: AGGACACCAGCTCTTTCACCCAC R: AGAGCAGCCCCTCAGCGTT
Fibroblast growth factor 18(FGF18)	F: CCCTGATGTCGGCCAAGTACTCT R: CTTCTGCAGCTCGGCCTGT
Fibroblast growth factor 22(FGF22)	F: GGCGCCGCGGGGACACCA R: CGCCAACGCACGTCGCCCT
Fibroblast growth factor receptor 1 (FGFR1)	F: TGCAAGGTGTACAGCGACCC R: CCTCCATCTCTTTGTCGGTGGTG
Fibroblast growth factor receptor 3(FGFR3)	F: CTGCCCGCCAACCAGACCG R: CCCACCTTGCTGCCGTTCACC

[a]:F, forward primer; [b]:R, reverse primer

Table S2.- KEGG classifications of unigenes.

No	Pathway	Count	Pathway ID
1	Metabolic pathways	2325	ko01100
2	Focal adhesion	1570	ko04510
3	Amoebiasis	1399	ko05146
4	Regulation of actin cytoskeleton	1241	ko04810
5	ECM-receptor interaction	1111	ko04512
6	Pathways in cancer	1059	ko05200
7	Protein digestion and absorption	975	ko04974
8	RNA transport	820	ko03013
9	MAPK signaling pathway	735	ko04010
10	Fc gamma R-mediated phagocytosis	697	ko04666
11	Adherens junction	690	ko04520
12	Endocytosis	676	ko04144
13	Chemokine signaling pathway	675	ko04062
14	mRNA surveillance pathway	604	ko03015
15	Spliceosome	596	ko03040
16	Tight junction	595	ko04530
17	Vascular smooth muscle contraction	581	ko04270
18	Huntington's disease	556	ko05016
19	Bacterial invasion of epithelial cells	553	ko05100
20	Dilated cardiomyopathy	551	ko05414
21	Pathogenic Escherichia coli infection	537	ko05130
22	Viral myocarditis	525	ko05416
23	Calcium signaling pathway	519	ko04020
24	Shigellosis	513	ko05131
25	Protein processing in endoplasmic reticulum	502	ko04141
26	Axon guidance	502	ko04360
27	Salivary secretion	498	ko04970
28	Phagosome	495	ko04145
29	Influenza A	492	ko05164
30	Wnt signaling pathway	488	ko04310
31	Purine metabolism	479	ko00230
32	Tuberculosis	469	ko05152
33	Ubiquitin mediated proteolysis	456	ko04120
34	Hypertrophic cardiomyopathy (HCM)	455	ko05410
35	Lysine degradation	451	ko00310
36	Vibrio cholerae infection	438	ko05110
37	Measles	423	ko05162
38	Insulin signaling pathway	413	ko04910
39	Leukocyte transendothelial migration	391	ko04670
40	Neurotrophin signaling pathway	382	ko04722
41	Alzheimer's disease	378	ko05010
42	Small cell lung cancer	369	ko05222
43	Toxoplasmosis	354	ko05145
44	Cell adhesion molecules (CAMs)	352	ko04514
45	B cell receptor signaling pathway	347	ko04662
46	Phosphatidylinositol signaling system	333	ko04070
47	Cell cycle	332	ko04110
48	Osteoclast differentiation	329	ko04380
49	Glutamatergic synapse	329	ko04724
50	Natural killer cell mediated cytotoxicity	328	ko04650
51	Cardiac muscle contraction	327	ko04260
52	GnRH signaling pathway	306	ko04912
53	Gastric acid secretion	305	ko04971
54	Basal transcription factors	298	ko03022
55	T cell receptor signaling pathway	295	ko04660
56	Hepatitis C	293	ko05160
57	Oocyte meiosis	293	ko04114
58	Fc epsilon RI signaling pathway	287	ko04664
59	Cytokine-cytokine receptor interaction	287	ko04060
60	Melanogenesis	285	ko04916
61	Cholinergic synapse	278	ko04725
62	Lysosome	275	ko04142
63	Prostate cancer	271	ko05215
64	Pyrimidine metabolism	270	ko00240
65	Hematopoietic cell lineage	262	ko04640
66	Gap junction	254	ko04540
67	Jak-STAT signaling pathway	254	ko04630
68	ErbB signaling pathway	250	ko04012
69	Ribosome biogenesis in eukaryotes	248	ko03008
70	Neuroactive ligand-receptor interaction	248	ko04080
71	Staphylococcus aureus infection	248	ko05150
72	TGF-beta signaling pathway	246	ko04350
73	VEGF signaling pathway	240	ko04370
74	Arrhythmogenic right ventricular cardiomyopathy (ARVC)	239	ko05412
75	Inositol phosphate metabolism	236	ko00562
76	Chagas disease (American trypanosomiasis)	235	ko05142
77	Leishmaniasis	234	ko05140
78	Pancreatic secretion	234	ko04972
79	Progesterone-mediated oocyte maturation	231	ko04914
80	Parkinson's disease	228	ko05012
81	Systemic lupus erythematosus	224	ko05322
82	RNA degradation	224	ko03018
83	p53 signaling pathway	221	ko04115
84	Apoptosis	210	ko04210
85	Glycerophospholipid metabolism	209	ko00564
86	Rheumatoid arthritis	208	ko05323

87	Amyotrophic lateral sclerosis (ALS)	205	ko05014
88	Oxidative phosphorylation	203	ko00190
89	Long-term potentiation	201	ko04720
90	Chronic myeloid leukemia	201	ko05220
91	Toll-like receptor signaling pathway	199	ko04620
92	Renal cell carcinoma	195	ko05211
93	Peroxisome	191	ko04146
94	Dorso-ventral axis formation	191	ko04320
95	Long-term depression	191	ko04730
96	Primary immunodeficiency	188	ko05340
97	Pancreatic cancer	182	ko05212
98	Glioma	181	ko05214
99	Colorectal cancer	180	ko05210
100	Adipocytokine signaling pathway	180	ko04920
101	Complement and coagulation cascades	177	ko04610
102	Basal cell carcinoma	175	ko05217
103	Acute myeloid leukemia	169	ko05221
104	Endometrial cancer	166	ko05213
105	Non-small cell lung cancer	165	ko05223
106	PPAR signaling pathway	163	ko03320
107	mTOR signaling pathway	162	ko04150
108	Bile secretion	160	ko04976
109	Notch signaling pathway	159	ko04330
110	Antigen processing and presentation	158	ko04612
111	Prion diseases	156	ko05020
112	African trypanosomiasis	153	ko05143
113	Hedgehog signaling pathway	152	ko04340
114	Epithelial cell signaling in Helicobacter pylori infection	150	ko05120
115	Type II diabetes mellitus	150	ko04930
116	NOD-like receptor signaling pathway	148	ko04621
117	ABC transporters	147	ko02010
118	Pertussis	146	ko05133
119	Ribosome	146	ko03010
120	RIG-I-like receptor signaling pathway	142	ko04622
121	Melanoma	139	ko05218
122	Aldosterone-regulated sodium reabsorption	139	ko04960
123	Endocrine and other factor-regulated calcium reabsorption	136	ko04961
124	Carbohydrate digestion and absorption	126	ko04973
125	Intestinal immune network for IgA production	125	ko04672
126	Arginine and proline metabolism	123	ko00330
127	Autoimmune thyroid disease	121	ko05320
128	Glycerolipid metabolism	121	ko00561
129	Glycolysis / Gluconeogenesis	119	ko00010
130	Vasopressin-regulated water reabsorption	119	ko04962
131	Cytosolic DNA-sensing pathway	116	ko04623
132	Valine, leucine and isoleucine degradation	116	ko00280
133	Allograft rejection	116	ko05330
134	Olfactory transduction	116	ko04740
135	N-Glycan biosynthesis	115	ko00510
136	Mineral absorption	113	ko04978
137	Phototransduction - fly	112	ko04745
138	RNA polymerase	110	ko03020
139	Nucleotide excision repair	109	ko03420
140	Bladder cancer	109	ko05219
141	Malaria	105	ko05144
142	Tyrosine metabolism	104	ko00350
143	Aminoacyl-tRNA biosynthesis	104	ko00970
144	Arachidonic acid metabolism	103	ko00590
145	Fat digestion and absorption	100	ko04975
146	Asthma	96	ko05310
147	Citrate cycle (TCA cycle)	95	ko00020
148	Other types of O-glycan biosynthesis	93	ko00514
149	Fatty acid metabolism	92	ko00071
150	Amino sugar and nucleotide sugar metabolism	91	ko00520
151	Fructose and mannose metabolism	91	ko00051
152	Thyroid cancer	90	ko05216
153	Ether lipid metabolism	90	ko00565
154	Tryptophan metabolism	88	ko00380
155	Taste transduction	84	ko04742
156	Vitamin digestion and absorption	83	ko04977
157	Base excision repair	83	ko03410
158	Pyruvate metabolism	82	ko00620
159	Sphingolipid metabolism	80	ko00600
160	Homologous recombination	80	ko03440
161	DNA replication	77	ko03030
162	Glutathione metabolism	76	ko00480
163	Cysteine and methionine metabolism	75	ko00270
164	SNARE interactions in vesicular transport	74	ko04130
165	Drug metabolism - cytochrome P450	71	ko00982
166	Glycosylphosphatidylinositol(GPI)-anchor biosynthesis	71	ko00563
167	Propanoate metabolism	70	ko00640
168	Histidine metabolism	67	ko00340
169	Glycine, serine and threonine metabolism	67	ko00260
170	Retinol metabolism	65	ko00830
171	beta-Alanine metabolism	63	ko00410
172	Starch and sucrose metabolism	63	ko00500
173	Drug metabolism - other enzymes	62	ko00983
174	Pentose phosphate pathway	62	ko00030
175	Collecting duct acid secretion	61	ko04966
176	Butanoate metabolism	61	ko00650
177	Proteasome	61	ko03050
178	Circadian rhythm - mammal	60	ko04710
179	Metabolism of xenobiotics by cytochrome P450	58	ko00980
180	Phototransduction	58	ko04744
181	Biosynthesis of unsaturated fatty acids	55	ko01040
182	Alanine, aspartate and glutamate metabolism	55	ko00250
183	Linoleic acid metabolism	54	ko00591
184	Nicotinate and nicotinamide metabolism	53	ko00760
185	Proximal tubule bicarbonate reclamation	53	ko04964
186	Mismatch repair	52	ko03430
187	alpha-Linolenic acid metabolism	52	ko00592
188	Porphyrin and chlorophyll metabolism	50	ko00860
189	Type I diabetes mellitus	50	ko04940
190	Regulation of autophagy	47	ko04140
191	Graft-versus-host disease	47	ko05332
192	Galactose metabolism	46	ko00052
193	Steroid hormone biosynthesis	46	ko00140
194	Glycosaminoglycan biosynthesis - chondroitin sulfate	43	ko00532
195	MAPK signaling pathway - fly	43	ko04013
196	Mucin type O-Glycan biosynthesis	42	ko00512
197	Non-homologous end-joining	42	ko03450
198	Glycosaminoglycan biosynthesis -	41	ko00534

	heparan sulfate		
199	Nitrogen metabolism	40	ko00910
200	Circadian rhythm - fly	39	ko04711
201	Selenocompound metabolism	37	ko00450
202	One carbon pool by folate	37	ko00670
203	Protein export	36	ko03060
204	Primary bile acid biosynthesis	36	ko00120
205	Glyoxylate and dicarboxylate metabolism	35	ko00630
206	Other glycan degradation	35	ko00511
207	Glycosaminoglycan degradation	34	ko00531
208	Pantothenate and CoA biosynthesis	32	ko00770
209	Steroid biosynthesis	31	ko00100
210	Renin-angiotensin system	31	ko04614
211	Pentose and glucuronate interconversions	30	ko00040
212	Glycosphingolipid biosynthesis - lacto and neolacto series	29	ko00601
213	Valine, leucine and isoleucine biosynthesis	29	ko00290
214	Glycosaminoglycan biosynthesis - keratan sulfate	27	ko00533
215	Phenylalanine metabolism	27	ko00360
216	Sulfur relay system	25	ko04122
217	Folate biosynthesis	24	ko00790
218	Ascorbate and aldarate metabolism	23	ko00053
219	Riboflavin metabolism	22	ko00740
220	Fatty acid elongation	22	ko00062
221	Terpenoid backbone biosynthesis	18	ko00900
222	Sulfur metabolism	17	ko00920
223	Maturity onset diabetes of the young	17	ko04950
224	Glycosphingolipid biosynthesis - ganglio series	16	ko00604
225	Glycosphingolipid biosynthesis - globo series	16	ko00603
226	Fatty acid biosynthesis	15	ko00061
227	Taurine and hypotaurine metabolism	15	ko00430
228	Vitamin B6 metabolism	14	ko00750
229	Lysine biosynthesis	13	ko00300
230	Synthesis and degradation of ketone bodies	13	ko00072
231	Thiamine metabolism	9	ko00730
232	Ubiquinone and other terpenoid-quinone biosynthesis	9	ko00130
233	Cyanoamino acid metabolism	9	ko00460
234	D-Glutamine and D-glutamate metabolism	7	ko00471
235	Caffeine metabolism	7	ko00232
236	D-Arginine and D-ornithine metabolism	6	ko00472
237	Butirosin and neomycin biosynthesis	6	ko00524
238	Phenylalanine, tyrosine and tryptophan biosynthesis	5	ko00400
239	Biotin metabolism	5	ko00780
240	Lipoic acid metabolism	4	ko00785
241	Polyketide sugar unit biosynthesis	2	ko00523

Table S3.- Growth factors identified in regenerating velvet skin of Red deer (*Cervus elaphus*) antlers. List of gene names and RPKM for 44 growth factor genes identified by RNA-Seq analysis from regenerating antler velvet skin.

Gene name of growth factor	RPKM[a]
Insulin-like growth factor 2 isoform 3	108.15
Transforming growth factor beta-1	76.31
Connective tissue growth factor	67.43
Heparin-binding growth factor 8	57.01
Hepatoma-derived growth factor	51.12
Vascular endothelial growth factor B	36.83
Stem cell growth factor	30.86
Erv1-like growth factor-like	23.05
PREDICTED: platelet-derived growth factor D isoform 2, partial	22.22
Transforming growth factor beta-3	21.53
Multiple epidermal growth factor-like domains 6-like	19.29
Fibroblast growth factor 7	19.03
Platelet-derived growth factor subunit A	18.26
Vascular endothelial growth factor	13.23
Platelet-derived growth factor subunit B	12.78
Hepatoma-derived growth factor 2-like protein	10.58
Growth differentiation factor-1/3	10.48
PREDICTED: multiple epidermal growth factor-like domains protein 9-like	9.07
PREDICTED: multiple epidermal growth factor-like domains protein 8, partial	8.97
Transforming growth factor beta-2	8.86
PREDICTED: platelet-derived growth factor subunit B-like	7.44
Adrenomedullin	6.74
Angiopoietin-1	6.60
Fibroblast growth factor 11	5.67
Epidermal growth factor-like protein 9	4.94
Angiopoietin-2	4.39
Vascular endothelial growth factor 120	4.36
Hepatocyte growth factor-like protein	4.25
Fibroblast growth factor 22	3.96
Stem cell factor	3.94
Fibroblast growth factor 9-like	3.61
Epidermal growth factor-like protein 7	3.44
Vascular endothelial growth factor D	3.23
Hepatocyte growth factor	3.21
Fibroblast growth factor 10	3.19
Transforming growth factor, alpha	3.08
PREDICTED: putative heparin-binding growth factor 1-like, partial	2.82
Growth differentiation factor-8/11	2.00
Fibroblast growth factor 18	1.93
Insulin-like growth factor I variant 4	1.71
Fibroblast growth factor 5	1.30
Angiopoietin-4	1.12
Glial cell line-derived neurotrophic factor	0.97
Growth differentiation factor-9	0.77

[a]Refers to reads per kilobase per million mapped reads

Table S4.- Growth factors receptors identified in regenerating velvet skin of Red deer (*Cervus elaphus*) antlers. List of gene names and RPKM for 26 growth factor receptor genes identified by RNA-Seq analysis from regenerating antler velvet skin.

Gene name of growth factor receptor	RPKM[a]
Platelet-derived growth factor receptor-like protein	55.18
Platelet-derived growth factor receptor, beta polypeptide	54.32
Autocrine motility factor receptor	38.02
Transforming growth factor beta type 2 receptor	30.48
Epidermal growth factor receptor	21.15
Nerve growth factor receptor	21.09
Insulin-like growth factor 2 receptor	20.74
PREDICTED: basic fibroblast growth factor receptor 1 isoform 3	17.07
Vascular endothelial growth factor receptor 2	16.65
Platelet-derived growth factor receptor,alpha polypeptide	14.31
Opioid growth factor receptor	12.80
BDNF/NT-3 growth factors receptor	12.60
Transforming growth factor beta type 3 receptor	12.12
PREDICTED: epidermal growth factor receptor substrate 15-like 1	9.56
Fibroblast growth factor receptor 3	8.77
Angiopoietin-1 receptor	5.57
Opioid growth factor receptor-like 1-like	4.74
Fibroblast growth factor receptor 1	4.69
Vascular endothelial growth factor receptor 1 isoform 2	3.76
Transforming growth factor beta type 1 receptor	3.58
Vascular endothelial growth factor receptor 1	3.26
PREDICTED: mast/stem cell growth factor receptor-like	3.22
Hepatocyte growth factor receptor	2.90
Erythropoietin receptor	2.28
Insulin-like growth factor 1 receptor	1.55
Fibroblast growth factor receptor 2	0.37

[a]Refers to reads per kilobase per million mapped reads.

SUPPLEMENTARY FIGURES LEGENDS

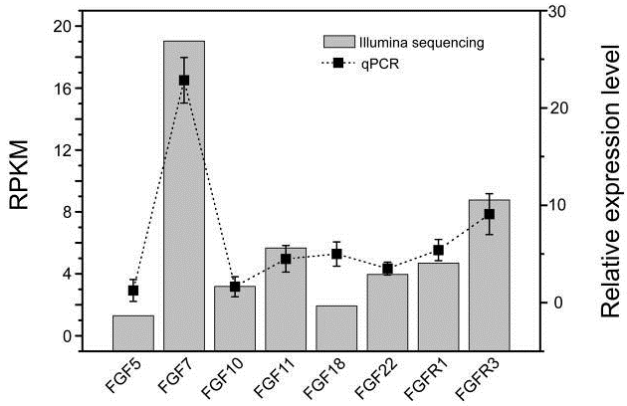

Fig. S1. Validation of growth factor and growth factor receptor genes in antler velvet of the Red deer transcriptome by qPCR. The primary *y*-axis indicates the relative abundance of candidate genes in antler velvet resulting from qPCR. The secondary *y*-axis indicates gene expression levels of candidate genes according to RPKM calculation. Abundance of target genes was normalized relative to abundance of the 7SL RNA gene. Bars in each panel represent standard errors of the mean (n = 6).